ELSEVIER

Infrared Physics & Technology 38 (1997) 117–122

INFRARED PHYSICS & TECHNOLOGY

Far-infrared spectroscopy of localized states in indium doped PbTe and $Pb_{1-x}A_xTe$ ($A_x = Mn_{0.017}$; $Sn_{0.18}$) alloys

N. Romčević [a,*], Z.V. Popović [a], D.R. Khokhlov [b], W. König [c]

[a] *Institute of Physics, P.O. Box 57, 11001 Belgrade, Yugoslavia*

[b] *Low-Temperature Physics Department, Moscow State University, 117234 Moscow, Russia*

[c] *Max-Planck-Institut für Festkörperforschung, Heisenbergstrasse 1, 70569 Stuttgart, Germany*

Received 10 October 1996

Abstract

Far-infrared reflection spectra of indium doped PbTe single crystal as well as of $Pb_{1-x}A_xTe$ alloys ($A_x = Mn_{0.017}$; $Sn_{0.18}$) in the temperature range between 10 and 300 K are presented. Analysis of the spectra was made by a fitting procedure based on the model of coupled oscillators. At temperatures below $T = 200$ K, two additional modes appear, along with the modes which describe strong plasmon–LO phonon coupling. The first mode, at about 122 cm^{-1}, is a local impurity mode of indium which represents a population of metastable states due to the transfer of electrons from two-electron to one-electron metastable impurity states. The second mode at about 488 cm^{-1} we believe to appear as a consequence of the electron transfer from a stable impurity two-electron state to the conduction band.

PACS: 72.15.Gd; 71.28.+d; 78.50.Ge; 63.20.Pro

1. Introduction

Semiconductor alloys of type $A^{IV}B^{VI}$ doped with the group III elements (In, Ga, Tl) have been the subject of intensive research for the past two decades [1–4]. Particular attention has been paid to alloys doped with indium because of a number of interesting phenomena (persistent photoconductivity effect [5], long-term relaxation processes [6], Fermi level pinning effect [7]). Namely, the introduction of indium into the solid solution $Pb_{1-x}A_xTe$ (A = Sn, Mn) leads to the formation of an impurity level in the energy spectra of the alloy. If the concentration of indium is higher than the concentration of other impurities, then it leads to the Fermi level pinning at the impurity level [7]. With PbTe(In), the impurity level appears at about 70 meV above the bottom of the conduction band [5]. With an increase in concentration of SnTe, or MnTe in PbTe, the impurity level (and the Fermi level pinning) is shifted from the conduction band, first to the forbidden band, and then to the valence band. The metal–semiconductor transition for $Pb_{1-x}Sn_xTe$(In) [5] is at $x = 0.22$, and for $Pb_{1-x}Mn_xTe$(In) [3] at $x = 0.05$.

Because of the high concentration of free carriers [1], optical properties of these alloys have been investigated mainly on thin films [8,9]. For $Pb_{0.75}Sn_{0.25}Te$(In) [8], the plasma frequency decreases with the lowering of temperature to a critical value $T_c = 25$ K, and below T_c it increases with

* Corresponding author.

PII S1350-4495(96)00042-4

further decrease of the temperature. This unusual behavior is connected with the persistent photoconductivity effect [5].

In our earlier papers we analyzed the reflection spectra, in the far-infrared region, of the single crystal samples $Pb_{0.75}Sn_{0.25}Te$ doped with 0.5 and 1.2 at% In, and $Pb_{0.9}Mn_{0.1}Te$ doped with 0.5 at% In [10–12]. In these samples the Fermi level stabilization pinning occurs in the forbidden band. Analysis of the spectra was performed by means of a classical dielectric function with one added oscillator. In addition to the already known characteristics of the basic crystal [13], the existence of a local In-impurity mode was confirmed. This mode, as discussed in Ref. [12], represents a population of metastable states due to the transfer of electrons from two- to one-electron metastable impurity states. The formation of an energy barrier between the impurity states represents a condition for the appearance of the persistent photoconductivity effect and the long-term relaxation process. This mode was also registered in the Raman scattering spectra of PbTe(In) [14]. By extending this study to infrared reflection spectra of PbTe(In), $Pb_{0.82}Sn_{0.18}Te$(In) and $Pb_{0.983}Mn_{0.017}Te$(In) single crystal samples, in which the Fermi level is in the conduction band, we expect to get a complete picture of the In impurity states in PbTe based alloys.

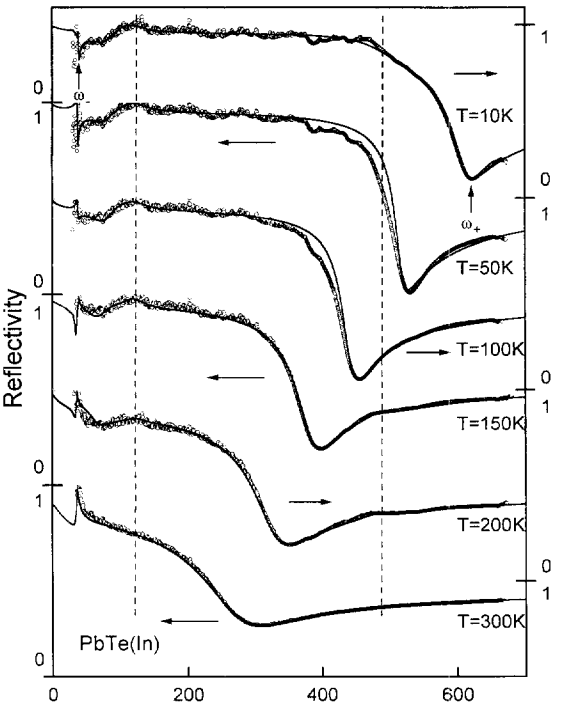

Fig. 1. Far-infrared reflection spectra of PbTe(In) single crystal. Experimental spectra are represented by circles. The solid lines are the calculated spectra obtained by a fitting procedure based on the model given by Eq. (1). Dashed vertical lines denote the position of ω_{0i} at 122 and 488 cm^{-1}.

2. Experiment

Single crystal samples of PbTe + 0.4 at% In, $Pb_{0.82}Sn_{0.18}Te$ + 0.3 at% In, and $Pb_{0.983}Mn_{0.017}Te$ + 0.2 at% In were grown using the Bridgeman technique. Details on the growth techniques can be found in Ref. [5].

A Bruker IFS 113v spectrometer with an Oxford cryostat was used to measure the far-infrared reflection spectra at low temperatures.

3. Results and discussion

The far-infrared reflection spectra of the indium doped PbTe single crystal sample and $Pb_{1-x}A_xTe$ ($A_xMn_{0.017}$; $Sn_{0.18}$) alloys are shown in Figs. 1–3. The experimental data are represented by circles. The solid lines were obtained using a modified factored dielectric function model of coupled plasmon–LO phonon modes [11,15]:

$$\varepsilon(\omega)=\varepsilon_\infty\left[\frac{\prod_{j=1}^{2}\left(\omega^2+i\gamma_{jl}\omega-\omega_{jl}^2\right)}{\omega\left(\omega+i\gamma_{\mathrm{P}}\right)\left(\omega^2+i\gamma_{\mathrm{t}}\omega-\omega_{\mathrm{t}}^2\right)}\times\frac{\omega^2+i\gamma_{\mathrm{LO}}\omega-\omega_{\mathrm{LO}}^2}{\omega^2+i\gamma_{\mathrm{TO}}\omega-\omega_{\mathrm{TO}}^2}+\sum_{k=1}^{2}\frac{\omega_{\mathrm{LOC}k}^2}{\omega^2+iG_k\omega-\omega_{0k}^2}\right] \quad (1)$$

where ω_{jl} and γ_{jl} represent the frequency and damp-

ing of the coupled plasmon–LO phonon modes; ω_t and γ_t are the frequency and damping of the transverse phonon mode; γ_P denotes the damping of plasmons and ε_∞ is the high-frequency dielectric constant. ω_{LO} and ω_{TO} are the longitudinal and transverse frequencies, and γ_{LO} and γ_{TO} stand for the dampings of uncoupled modes of the host crystal. The second term in Eq. (1) represents an In-impurity local mode and a mode that describes electron transfer from a stable two-electron state to the conduction band, to be discussed later. The characteristic parameters for the best fit of the model with the experimental results are shown in Figs. 4–6.

The oscillators denoted by $j = 1, 2$ in Eq. (1) are the dominant structures in the far-infrared spectra and represent the positions of the coupled plasmon–LO phonon modes. The frequencies of these modes ($\omega_\pm$) are marked by arrows in Fig. 1. The transverse

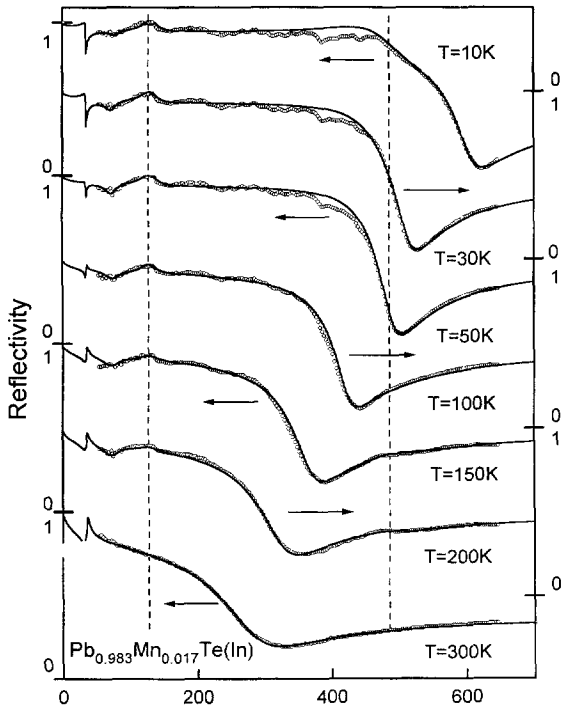

Fig. 2. Experimental (circles) and calculated (solid lines) far-infrared reflection spectra of $Pb_{0.983}Mn_{0.017}Te(In)$ single crystal. Dashed vertical lines denote the position of ω_{0i} at 122 and 488 cm^{-1}.

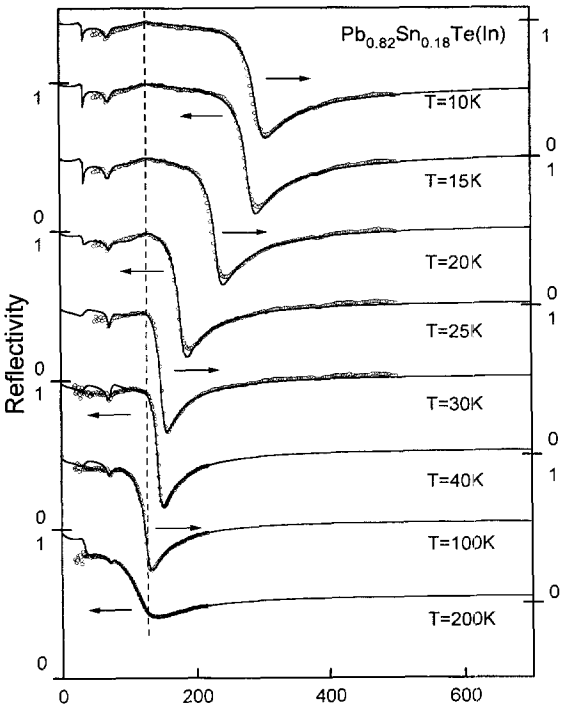

Fig. 3. Measured (circles) and calculated (solid lines) far-infrared reflection spectra of $Pb_{0.82}Sn_{0.18}Te(In)$ single crystal. Dashed vertical lines denote the position of ω_{0i} at 122 and 488 cm^{-1}.

phonon frequency ω_t, determined at about 34 cm^{-1}, is in good agreement with the literature [13].

An oscillator of a weak intensity, at about 70 cm^{-1} (the second member in the product), is a mode from the edge of the Brillouin zone, because the phonon density of PbTe [16] has a maximum at that frequency. This mode is already observed in many PbTe based alloys [11,12,17].

In Fig. 4, the points refer to the eigenfrequency spectra ω_{jl} obtained by Eq. (1). The values for ω_{LO} and ω_P were determined as described in Ref. [15]. The temperature change of ω_P is shown in the inset of Fig. 4. The plasma frequency ω_P increases as the temperature decreases, being a consequence of the appropriate change in the free carriers concentration of these alloys when the Fermi level is pinned in the conduction band [5,6]. The value obtained for ω_{LO} (104 cm^{-1}) is in agreement with the values found in the literature [13].

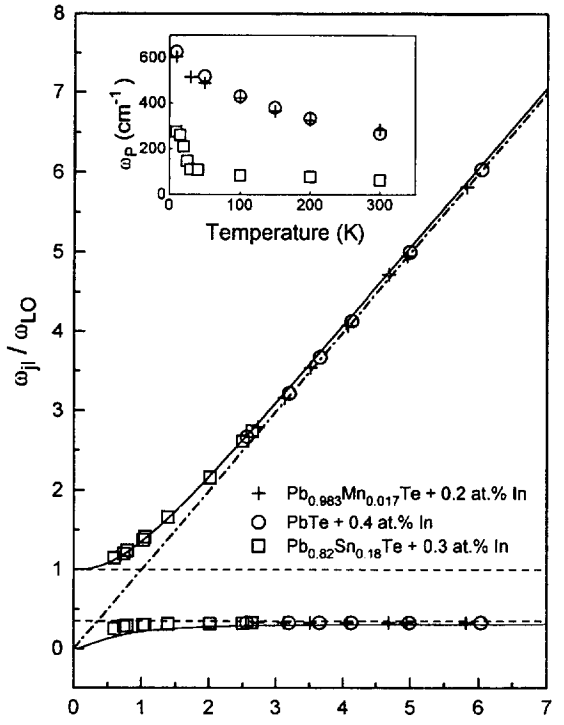

Fig. 4. The eigenfrequencies of the plasmon–phonon modes. Inset: Plasma-frequency–temperature dependences for three different samples.

The solid lines in Fig. 4 are obtained by application of [18]:

$$\omega_{\pm}^2 = \tfrac{1}{2}\left(\omega_P^2 + \omega_{LO}^2\right) \pm \left[\tfrac{1}{4}\left(\omega_P^2 + \omega_{LO}^2\right)^2 - \omega_P^2\omega_t^2\right]^{1/2}. \quad (2)$$

The agreement of the plasmon–LO phonon mode frequencies calculated on the basis of Eq. (2) with the experimentally determined ones is very well. In this manner it is shown that the dielectric function, Eq. (1), can be used in the case of paired coupled plasmon–LO phonon modes, to obtain the frequencies of coupled modes from the experiment, and then to calculate the values for ω_{LO} and ω_P.

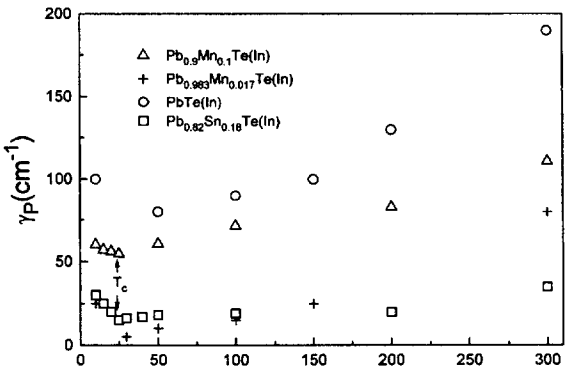

Fig. 5. Temperature dependence of the damping of plasmons γ_P.

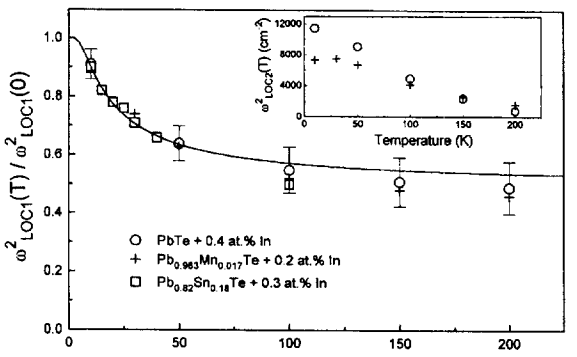

Fig. 6. Temperature dependence of normalized 'strength' $\omega^2_{LOC1}(T)/\omega^2_{LOC1}(0)$ of the additionally introduced oscillator at $\omega_{01} = 122$ cm^{-1}. Inset: Temperature dependence of 'strength' ω^2_{LOC2} of the additionally introduced oscillator at $\omega_{02} = 488$ cm^{-1}. Bars are absolute error values of $\omega^2_{LOC1}(T)/\omega^2_{LOC1}(0)$ obtained during the fitting procedure.

Fig. 5 illustrates the temperature dependence of the plasmon mode damping γ_P for PbTe(In), $Pb_{0.983}Mn_{0.017}Te$(In), $Pb_{0.82}Sn_{0.18}Te$(In) and $Pb_{0.9}Mn_{0.1}Te$(In) [12] samples. Decrease in temperature up to $T = 25$ K lowers the γ_P value, valid for all samples. Further decrease in temperature leads to an increase in γ_P. Such a change in γ_P is characteristic for all PbTe based alloys doped with In and Ga where the persistent photoconductivity effect is registered [4,8,11,12]. The critical temperature $T_c = 25$ K, determined in the way described, is in accordance with the results of the galvanomagnetic [1,3,5] and optical measurements [8,10–12].

At temperatures below $T = 200$ K (PbTe(In) and $Pb_{1-x}Mn_xTe$(In)), or $T = 100$ K ($Pb_{1-x}Sn_xTe$(In)), a new structure is observed (local maximum at about 122 cm^{-1}) in the reflection spectra (Figs. 1–3). In order to describe the structure, an oscillator is added to the dielectric function of Eq. (1), at these temperatures, with characteristic frequency ω_{01}, damping G_1 and 'strength' ω_{LOC1} of the additional oscillator. The characteristic frequency ($\omega_{01} = 122$ cm^{-1}) remains unchanged with the change in temperature, alloy content, and the In concentration, while the oscillator

strength falls abruptly at temperatures higher than $T_c = 25$ K.

Since the additional mode is of the same frequency for all reflection spectra, independent of the position of the Fermi level and content of the alloy, we conclude that this structure exhibits the same nature in all alloys and represents the impurity mode of indium.

On the other hand, due to a sudden increase in strength of the additional oscillator at temperatures lower than 25 K (Fig. 6), this mode represents a population of metastable one-electron impurity states due to the transfer of electrons from the stable two-electron state to the metastable one-electron state [14], which is discussed in more detail in Ref. [14].

Similar results were reported in our previously published papers [4,10–12] for the reflection spectra of lead–telluride-alloys doped with In and Ga with the impurity level in the forbidden band. In all cases, the appearance of a new structure is registered at the same frequency.

The population of these states is determined by the balance between photo excitation and recombination. We suppose that the main mechanism of recombination, at temperatures near and below T_c, is the thermal activation through the barrier E_b (see Fig. 7) which separates the stable from the metastable states. To make it simple, we assume that E_b does not change with the temperature (other cases of the position of barriers are discussed in Ref. [12]). Since the strength of the oscillator is proportional to the population of the metastable states, the following temperature dependence can be proposed [12]:

$$\omega_{LOC}^2(T) = \omega_{LOC}^2(0)\left(1 - \tfrac{1}{2}e^{-E_b/kT}\right). \quad (3)$$

The solid line in Fig. 6 was obtained by Eq. (3). Agreement of the experimental values and the proposed simple model at lower temperatures is rather good. Also, the value obtained for E_b is independent of the alloy content and indium concentration, and amounts to $E_b = 1.6$ meV. This value is lower than the values obtained up to now [11,12] in accordance with our expectations, since the effect of persistent photoconductivity in these alloys (in direct proportionality with E_b) is quite weaker comparing with the systems with the Fermi-level pinning inside the forbidden band.

In the reflection spectra (Figs. 1 and 2), at about 488 cm^{-1} and temperatures below $T = 200$ K, a new structure is observed. To describe this structure we added one more oscillator, shaped as in Ref. [19], to the dielectric function. The characteristic frequency of this oscillator is independent of the alloy content and temperature ($\omega_{02} = 488$ cm^{-1}). This, as before, leads us to conclude that the nature of this additional oscillator is connected with the characteristics of In in these systems.

As known, the neutral state of indium in the lattice (In^{2+}) is unstable [2] and according to

$$2In^{2+} = In^{+} + In^{3+}$$

transfers to the two-electron stable state (In^{+}), which is energy-wise more favorable than the metastable single-electron (In^{2+}) and the state of the empty center (In^{3+}).

Electrons from the In^{+} state transfer into the conduction band according to

$$In^{+} \rightarrow In^{3+} + 2e.$$

According to Ref. [2], the energy change at the impurity center is $\Delta E_2 = 60$ meV. Since such a predicted energy is very close to the experimentally determined one (61 meV), we believe that this oscillator is a result of the electron transfer from the two-electron impurity state to the conduction band. In favor of this is the fact that the intensity of this oscillator increases as temperature decreases (see

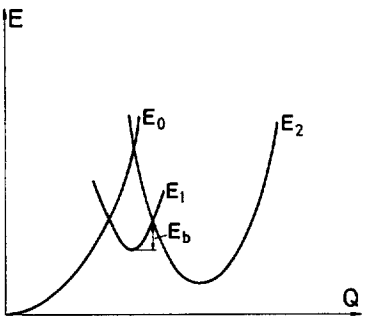

Fig. 7. Configuration coordinate diagram for indium in PbTe based alloys when the Fermi level is pinned in the conduction band.

inset in Fig. 6). As a consequence, there is an increase in the free carriers concentration, which is experimentally confirmed.

4. Conclusion

In this paper we have shown the far-infrared reflection spectra of indium doped PbTe single crystal and $Pb_{1-x}A_xTe$ ($A_x = Mn_{0.017}$; $Sn_{0.18}$) alloy samples at temperatures between 10 and 300 K. In addition to the strong plasmon–LO phonon interaction, characteristic for these alloys, two additional modes at temperatures below $T = 200$ K are observed. The first mode, at about 122 cm^{-1} is the local vibrational indium impurity mode representing the population of a metastable state due to the transfer of electrons from a stable two-electron to a metastable one-electron state. The other mode, at about 488 cm^{-1} may be a result of electron transfer from the stable impurity two-electron state to the conduction band.

Acknowledgements

This work is supported by the Serbian Ministry of Science and Technology under project 01E09.

References

[1] B.A. Akimov, N.B. Brandt, L.I. Ryabova, V.V. Sokovishin and S.M. Chudinov, J. Low Temp. Phys. 51 (1993) 9.

[2] M. Vul, I.S. Voronova, G.M. Kalyzhnaya, T.S. Mamedov and T.S. Ragimova, Pism'ma v ZETF 29 (1979) 21 [JETP Lett. 29 (1979) 18].

[3] B.A. Akinov, A.V. Nikorich, L.I. Ryabova and N.A. Shirokova, Fiz. Tekh. Poluprovodn. 23 (1989) 1019 [Sov. Phys. Semicond. 23 (1989) 748].

[4] A.L. Belogorok11ov, S.A. Belokon', I.I. Ivanchik and D.R. Khokhlov, Fiz. Tverd. Tela 34 (1992) 1651 [Sov. Phys. Solid State 34 (1992) 2966].

[5] B.A. Akimov, L.I. Ryabova, O.B. Yatsenko and S.M. Chudinov, Fiz. Tekh. Poluprovodn. 13 (1979) 752 [Sov. Phys. Semicond. 13 (1979) 441].

[6] I.I. Zasavitskiy, A.B. Matveenko, B.N. Matsonashvili and V.T. Trofimov, Fiz. Tekh. Poluprovodn. 21 (1987) 1789 [Sov. Phys. Semicond. 21 (1987) 1084].

[7] B.A. Akimov, N.B. Brandt, S.O. Klimonskiy, L.I. Ryabova and D.R. Khokhlov, Phys. Lett. A 88 (1982) 483.

[8] S.W. McKnight and M.K. El-Rayess, Solid State Commun. 49 (1984) 1001.

[9] K.S. Takaoka, T. Itoga and K. Murase, Jpn. J. Appl. Phys. 23 (1984) 216.

[10] N. Romčević, Z.V. Popović, D.R. Khokhlov, A.V. Nikorich and W. König, Phys. Rev. B 43 (1991) 6712.

[11] N. Romčević, Z.V. Popović and D.R. Khokhlov, J. Phys.: Condens. Matter 4 (1992) 4323.

[12] N. Romčević, Z.V. Popović, D.R. Khokhlov, I.I. Ivanchik, A.V. Nikorich and W. König, unpublished.

[13] Yu.I. Ravich, B.A. Efimova and I.A. Smirnov, Semiconducting Lead Chalogenides, ed. L.S. Stil'bans (Plenum, New York, 1970).

[14] N. Romčević, Z.V. Popović and D.R. Khokhlov, J. Phys.: Condens. Matter 7 (1995) 5105.

[15] A.A Kukharskii, Solid State Commun. 13 (1973) 1761.

[16] W. Cochran, R.A. Cowley, G. Dolling and M.M. Elcombe, Proc. R. Soc. A 293 (1966) 433.

[17] J.M. Miljković, N. Romčević, Z.V. Popović, W. König, and V.N. Nikiforov, Phys. Status Solidi (b) 193 (1996) 43.

[18] M. Cardona, ed., Light Scattering in Solids; Topics Appl. Phys., Vol. 8 (Springer, Berlin, Heidelberg, New York, 1975 and 1982).

[19] Yu.A. Pusep and M.P. Sinyukov, Pis'ma v ZETF 45 (1987) 449 [Sov. Phys. JETP Lett. 45 (1987) 577].